ELSEVIER

Catalysis Today 78 (2003) 397–409

CATALYSIS TODAY

www.elsevier.com/locate/cattod

Niobium oxide as support material for the oxidative dehydrogenation of propane

Maymol Cherian, Musti Someswara Rao, Goutam Deo*

Department of Chemical Engineering, Indian Institute of Technology, Kanpur 208-016, India

Abstract

The ability of using niobium oxide (Nb_2O_5) as a support for preparing surface metal oxide species and testing the catalyst for the ODH of propane was done in the present study. Chromium oxide was used as the representative surface metal oxide species. To test the objective several loadings of Cr_2O_3/Nb_2O_5 were prepared by the incipient wetness impregnation technique. Surface area analysis, Raman, X-ray photoelectron spectroscopy (XPS) and electron paramagnetic resonance (EPR) spectroscopy and TPR studies were used to characterize the sample. It was observed that surface chromium oxide species are formed similar to those on other oxide supports and similar monolayer coverages were achieved. However, the reduction characteristic (T_{max} temperature) was different due to the change in the Cr–O–support bond. The ODH of propane over the Cr_2O_3/Nb_2O_5 catalysts revealed that the activity increased up to monolayer coverage and then decreased due to the presence of Cr_2O_3 crystals. Similar observations were seen for the V_2O_5/Nb_2O_5 and MoO_3/Nb_2O_5 catalysts. The turnover frequency (TOF) was independent of coverage for the surface chromium, vanadium and molybdenum oxide species on Nb_2O_5. The constant TOF suggests the structure insensitivity of this type of reaction. The propene selectivities were high and relatively constant for the Cr_2O_3/Nb_2O_5 catalysts revealing the higher yields that can be obtained on this series of catalysts compared to the Cr_2O_3/Al_2O_3 and Cr_2O_3/TiO_2 catalysts. Additional studies involving tungsten and molybdenum oxide additives on 1% Cr_2O_3/Nb_2O_5 reveal the effect of exposed support surface on the propene selectivities.

Keywords: Niobium oxide; Turnover frequency; ODH

1. Introduction

Supported metal oxide catalysts find a variety of applications in the petrochemical and environmental industries [1,2]. The commonly used supports for preparing supported metal oxide catalysts are Al_2O_3, SiO_2 and TiO_2. Supported metal oxides are formed when the active component, usually a transitional metal oxide, is dispersed on the surface of a high surface area oxide-support to form two-dimensional overlayers or surface species. Past research suggests that the oxide support should be of reasonable high surface area, stable for supporting the active surface species and thermally stable under reaction conditions. Essentially, the support should provide the required physical and chemical properties necessary for the active species to maintain a high activity during reaction.

In addition to being used as a promoter, niobium oxide (Nb_2O_5) has also been used successfully as a support for preparing supported metal oxide catalysts [3]. It was shown that Nb_2O_5 could be used to form

---

* Corresponding author. Tel.: +91-512-597881;
fax: +91-512-590104.
E-mail address: goutam@iitk.ac.in (G. Deo).

PII: S0920-5861(02)00306-1

two-dimensional overlayers of vanadium, chromium, rhenium, molybdenum, and tungsten oxides. These Nb_2O_5 supported metal oxides were successfully tested for the partial oxidation of methanol. It was observed that these Nb_2O_5 supported catalysts were able to convert methanol to formaldehyde with turnover frequencies comparable to, or better than, other supported metal oxide catalysts that used more traditional supports, such as Al_2O_3, SiO_2 and TiO_2. For example, the turnover frequency (TOF) for the V_2O_5/Nb_2O_5 catalysts ($\sim 0.7\,s^{-1}$) were comparable to the V_2O_5/TiO_2 catalysts ($\sim 1.8\,s^{-1}$) and much better than the TOF for the V_2O_5/Al_2O_3 or V_2O_5/SiO_2 catalysts [4]. Based on these and other studies it would appear that Nb_2O_5 supported metal oxide catalysts are promising materials for oxidation reactions [5,6].

The oxidative dehydrogenation (ODH) of propane to propene is a reaction of considerable importance. Several supported metal oxides have been successfully tested with varying degrees of success. Considering the ODH of propane to be essentially a redox reaction it would appear worthwhile that Nb_2O_5 supported metal oxides be studied to access the advantages/disadvantages of using these types of catalysts. There are a few studies that exist for the application of Nb_2O_5 supported metal oxides for the ODH of propane. Watling et al. [7] studied the effect of loading and preparation method for V_2O_5/Nb_2O_5 catalysts and suggested that the TOF for the ODH of propane reaction was essentially independent of coverage for the surface vanadium oxide species. Zhao and Wachs [8] revealed that the V_2O_5/Nb_2O_5 and MoO_3/Nb_2O_5 catalysts could also be used for the ODH of propane and the TOFs were also essentially independent of coverage. Furthermore, the TOFs for the V_2O_5/Nb_2O_5 catalysts were greater than those obtained for the MoO_3/Nb_2O_5 catalysts.

In the present study the ODH of propane using Nb_2O_5 supported metal oxides is discussed. Special attention is given to the surface chromium oxide species since, to the best of our knowledge, the Cr_2O_3/Nb_2O_5 catalyst has not been used for the ODH of propane. The activity and propene selectivity of the surface chromium oxide species on Nb_2O_5 will be compared to those on other oxide supports. Furthermore, the effect of tungsten and molybdenum oxide additives will also be considered to bring out any similarities or difference with other modified supported metal oxide catalysts.

2. Experimental

2.1. Catalyst preparation

Niobium supported chromium oxide catalysts were prepared by the incipient wetness impregnation technique. The precursor used was chromium nitrate nanohydrate ($Cr(NO_3)_3 \cdot 9H_2O$, Aldrich, 99.98% purity). The Nb_2O_5 support was obtained from Niobium Products Company (CBMM). The support was pretreated with incipient volumes of distilled water and then calcined at 723 K for 6 h. The pretreated support and incipient volumes of solution containing predetermined amounts of precursor were intimately mixed in order to prepare the catalysts with different loadings of chromium oxide. The mixture was kept in a dessicator overnight followed by drying at 383 K for 8 h, and then calcined at 523 K for another 8 h. Finally, the samples were calcined at 723 K for 6 h. The prepared catalysts were denoted as x% CrNb, where x% is the wt.% loading in terms of Cr_2O_3.

The CrNb catalysts were modified with molybdenum and tungsten oxides additives (denoted as MoO_3 and WO_3). The modified catalysts were prepared by a two-step impregnation procedure. Initially, a 1% CrNb sample was prepared by the procedure given above and then this sample was modified with the additives. The precursors used for the molybdenum and tungsten oxide additives were ammonium hepta-molybdate ($(NH_4)_6Mo_7O_{24} \cdot 2H_2O$, Alfa products) and ammonium meta tungstate ($(NH_4)_6H_2W_{12}O_{40}$), respectively. An aqueous solution of required amount of precursors for preparing 2 wt.% MoO_3 and 4 wt.% WO_3 were introduced into the previously prepared 1% CrNb catalyst. The precursor solution and 1% CrNb catalyst were thoroughly mixed and subjected to the same heat treatment as above. The modified samples were denoted as CrNb–4% W and CrNb–2% Mo. Unmodified 2% MoO_3/Nb_2O_5 and 4% WO_3/Nb_2O_5 were also prepared by impregnating the pretreated Nb_2O_5 support using the required amount of aqueous solution of the precursors and following similar heat treatment procedures as above and denoted as MoNb and WNb, respectively.

2.2. Surface area

The surface areas of the samples were obtained using the single point BET method. A bench-top COULTER SA 3100 apparatus using N_2 adsorption at 77 K was used for this purpose.

2.3. Raman spectroscopy

The laser Raman spectroscopy study of the series of CrNb samples under ambient conditions were obtained by means of an argon ion laser (Spectra Physics, Model 165). About 200 mg of the supported chromia catalysts were pressed into self-supporting wafers and placed in a rotating sample cell to avoid local heating effects. Additional details can be found elsewhere [9].

2.4. X-ray photoelectron spectroscopy (XPS)

XPS studies were done using Mg Kα or Al Kα in fixed analyzer transmission (FAT) mode. The catalyst powder was pressed between a stainless steel holder and a polished single crystal silicon wafer, which was then installed in a vacuum chamber of a Model DS 800 XPS surface analysis system.

2.5. Electron paramagnetic resonance (EPR)

EPR studies were performed on a Varian-E-109 X band spectrometer. The spectra were obtained at room temperature using a microwave frequency of ∼9.15 GHz and a microwave power of 10 mW. The scan time was 8 min and magnetic field modulation frequency was 100 kHz. The EPR spectra were calibrated with DPPH (α,α′-diphenyl-β-picryl hydrazyl) using a duel cell.

2.6. Temperature programmed reduction (TPR)

The TPR studies were carried out in a microreactor containing ca. 0.05 g of catalyst and attached to a Micromeritus Pulse Chemisorb 2705 analyzer. Helium was used as the carrier gas and also to degas the samples at 573 K for 0.5 h prior to the reduction experiments. The helium flow was set at 30 ml/min. A 10% H_2/Ar mixture flowing at 40 ml/min was used for reduction and the temperature was ramped at a rate of 10 K/min from ∼373 to 973 K. The amount of hydrogen consumed was detected using a TCD. Known amounts of pure hydrogen were injected for quantification purposes.

2.7. ODH of propane

The samples were tested for the ODH of propane in a vertical down-flow quartz reactor at atmospheric pressure. The reactor was a single quartz piece of inlet 10 mm internal diameter and 15 cm long, and outlet of 5 mm internal diameter and 15 cm long. The two sections were tapered and the catalyst bed was placed just above the tapered region on quartz wool. The reactor tube was mounted vertically in a tubular furnace. The temperature of the reactor and the catalyst bed was measured by a thermocouple located inside the reactor tube just above the catalyst bed and was controlled by a PID temperature controller (FUJI Micro-controller X Model PXZ 4). The product gases were sent for online analysis to a gas chromatograph (AIMIL–NUCON 5765) equipped with a methanizer. The carbon oxides and hydrocarbons are analyzed in FID mode using activated alumina column. The propane flow was adjusted through a separate thermal mass flow controller (Bronkhost Hi-Tec, Model F-201D FAC-22-V) and the air flow rate was adjusted through a rotameter (Eureka, Model SRS/MG-5) to maintain a 3:1 propane to oxygen ratio and a total flow rate of 42.7 sccm. A physical mixture of 0.1 g of the catalyst and required amount of quartz glass powder to form a bed height of 1 cm was loaded into the reactor. Runs were performed at different temperatures starting from 573 to 723 K. Conversions were maintained below 5% to ensure differential conditions.

Based on the inlet and outlet concentrations and assuming differential reactor conditions the conversion, activity, selectivity, yield and TOF were calculated as follows:

$$\text{Conversion (\%)} = \left(\frac{n_\text{c}}{n_\text{f}}\right) \times 100$$

$$\text{Activity} \left(\frac{\text{moles of C}_3\text{H}_8\text{ converted}}{\text{g s}}\right) = F_{\text{A}0} \times X_\text{A}$$

$$\text{Selectivity (\%)} = \left(\frac{n_\text{hc}}{n_\text{c}}\right) \times \left(\frac{N_\text{hc}}{N_\text{p}}\right) \times 100$$

$$\text{Yield (\%)} = \left(\frac{n_{hc}}{n_f}\right) \times \left(\frac{N_{hc}}{N_p}\right) \times 100$$

$$\text{TOF (s}^{-1}\text{)} = \frac{F_{A0} \times X_A}{n_{Cr}}$$

where n_c, n_f are the number of moles of propane consumed and propane fed, respectively; n_{hc} the number of moles of products (e.g. propene, ethene, carbon oxides, etc.) formed; and N_{hc} and N_p are the number of carbon atoms present in the products formed and propane, respectively; F_{A0} the moles of propane fed per second; X_A the conversion of propane per gram of the catalyst and n_{Cr} the moles of Cr per gram of the catalyst.

Blank reactor runs were conducted and no significant conversions were observed under the present experimental conditions. Pure Nb_2O_5 support, MoNb and WNb samples were observed to be inactive for the ODH of propane under the present experimental conditions. For each catalyst several runs were taken and the average value is reported.

3. Results

Several loadings of chromium oxide on niobium oxide were prepared. These samples were initially characterized in order to understand the nature of the supported chromium oxide phase. Characterization of the samples was achieved by analyzing the surface area and other data from Raman, XPS, EPR and TPR studies. The samples were then tested for the ODH of propane. The results of these studies are given below.

3.1. Surface area and surface concentration

Table 1
Surface areas and surface concentrations of Cr_2O_3/Nb_2O_5 samples

Sample	Surface area (m^2/g)	Surface concentration ($\mu mol\ Cr/m^2$)
Nb_2O_5	51	–
1% CrNb	36	3.7
3% CrNb	34	11.6
5% CrNb	30	21.9
7% CrNb	26	35.4
10% CrNb	26	50.6

The surface areas of the supported chromium oxide samples were determined and given in Table 1. The surface area values given in Table 1 reveal that the addition of chromium oxide reduces the surface area from 51 m^2/g for the pure Nb_2O_5 support to 26 m^2/g for the 7 and 10% CrNb samples. Based on the surface areas and chromium oxide loadings of the samples the surface concentrations ($\mu mol\ Cr/m^2$) were also determined and given in Table 1. It is observed that the surface concentration increases with the increase in chromium oxide loading from 3.7 $\mu mol\ Cr/m^2$ for the 1% CrNb sample to 50.6 $\mu mol\ Cr/m^2$ for the 10% CrNb sample.

3.2. Raman spectra

The Raman spectra of the CrNb samples obtained under ambient conditions are shown in Fig. 1 in the 400–1200 cm^{-1} region. A strong broad band was observed at 700 cm^{-1} due to the Nb_2O_5 support. Initial addition of chromium oxide to the Nb_2O_5 support gives rise to broad bands at 893–897 and 990–997 cm^{-1}, which correspond to Cr^{6+} species in monochromates and polychromates [10,11]. The intensity of these bands increase with loading up to 3% Cr_2O_3. For chromium oxide loadings above 3% Cr_2O_3 an additional band at 550 cm^{-1} is observed, which is due to bulk Cr_2O_3 [10]. The intensity of the 550 cm^{-1} band increases with additional chromium oxide loading.

Ambient Raman spectroscopic studies for CrNb–4% W and CrNb–2% Mo were also performed. Peaks due to surface chromium and tungsten oxide species appear at ~830 and 950 cm^{-1}, respectively, and surface chromium and molybdenum oxide species appear at ~850 and 970 cm^{-1}, respectively. The Raman spectra for modified CrNb catalysts were not shown for brevity.

3.3. XPS

The XPS studies on the CrNb samples revealed the presence of Cr, Nb, O and C. In addition, trace amounts of fluorine, chlorine and tin were also observed. Based on the atomic ratio of chromium and niobium determined from the XPS spectra, the $Cr/(Cr + Nb)_{surface}$ was calculated. Furthermore, based on the bulk

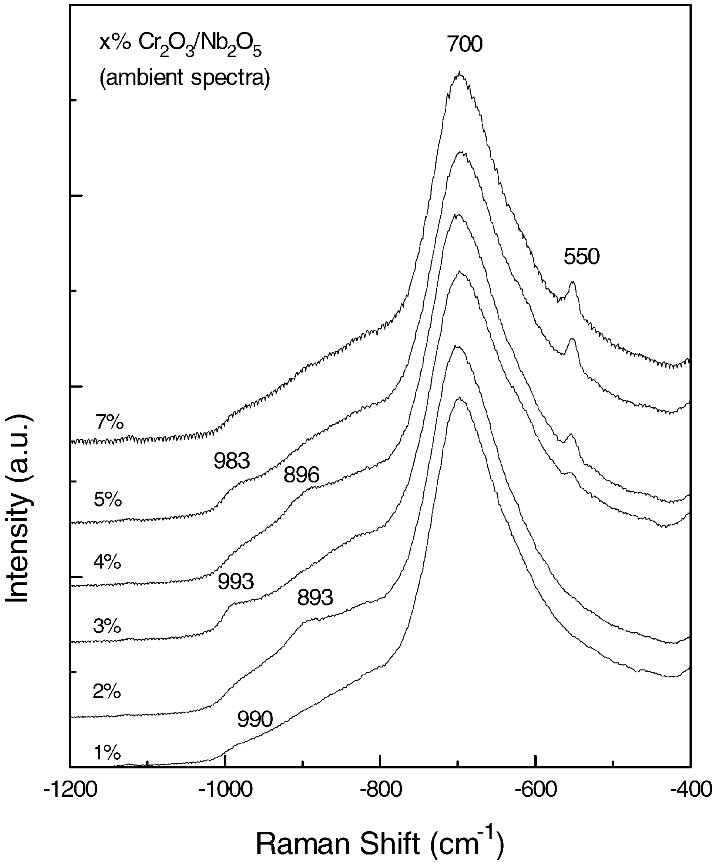

Fig. 1. Raman spectra of x% CrNb catalysts under ambient conditions ($x = 1$–7).

composition of the samples the $\mathrm{Cr/(Cr + Nb)_{bulk}}$ was also calculated. The $\mathrm{Cr/(Cr + Nb)_{surface}}$ was plotted versus $\mathrm{Cr/(Cr + Nb)_{bulk}}$ in Fig. 2. Fig. 2 reveals that the $\mathrm{Cr/(Cr + Nb)_{surface}}$ value initially increases with an increase in chromium oxide loading, i.e., $\mathrm{Cr/(Cr + Nb)_{bulk}}$ value, and then remains constant. Similar types of curves have been observed for chromium oxide on other oxide supports [12] and other supported metal oxide samples [13,14].

3.4. EPR spectra

The EPR spectra of the CrNb samples obtained under ambient conditions are shown in Fig. 3 as a function of chromium oxide loading. As the chromium oxide loading is increased a band is observed with a g-value of 1.97. The ΔH of this band increases from 120 to 140 G. Further addition of chromium oxide, till 3% Cr_2O_3 loading, results in the increase in intensity of this band with a g-value of 1.97. The band with a g-value of 1.97 has been assigned to a γ-Cr^{5+} species [15]. Above 3% Cr_2O_3 loading a broad feature develops with a g-value of 1.96 and $\Delta H =$ 700 G. The intensity of this band increases with further increase in wt.% of Cr_2O_3. This broad band corresponds to Cr^{3+} species (β-Cr^{3+}) due to Cr_2O_3 crystal [16].

The EPR spectra of the modified CrNb catalysts are also obtained. A single peak corresponding to γ-Cr^{5+} species with $g = 1.97$ and $\Delta H = 140$ was observed for CrNb–4% W and CrNb–2% Mo catalysts, however, the intensity of this peak was lower than that for the CrNb catalysts. Similar spectra were observed for tungsten modified CrTi catalysts [17].

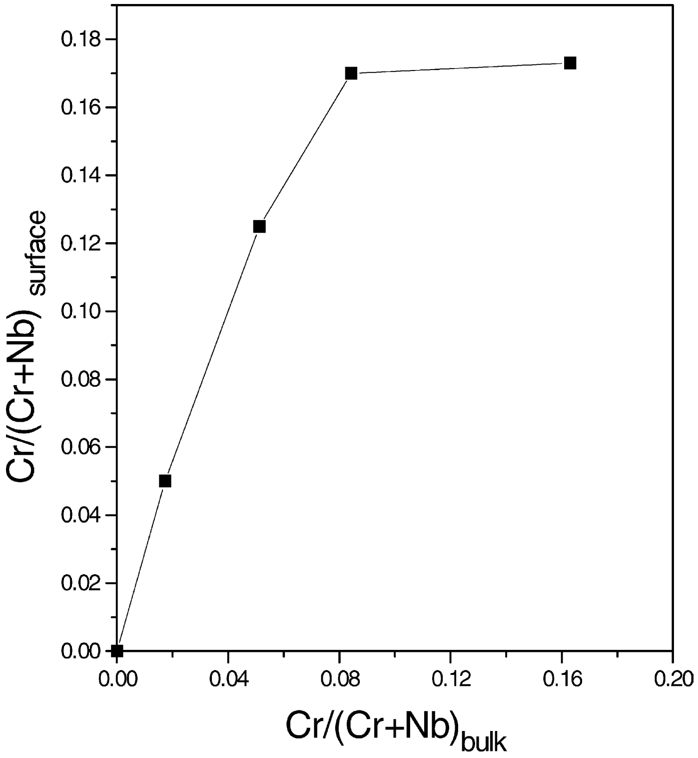

Fig. 2. $Cr/(Cr + Nb)_{surface}$ determined from XPS studies versus $Cr/(Cr + Nb)_{bulk}$ for the CrNb catalysts.

3.5. TPR

TPR studies of the 1–5% CrNb samples were also performed using hydrogen as the reductant, and the results are shown in Table 2. The TPR profiles of these CrNb samples reveal a single reduction peak. The position of the reduction peak, denoted as T_{max}, is given in Table 2. With an increase in chromium oxide loading it is observed that the T_{max} increases slightly from 588 to 599 K and then remains constant. The initial increase in T_{max}, however, is small and may be within experimental error. Based on the peak area and injection of known amounts of hydrogen the hydrogen consumption per gram of the samples was determined, which were then converted to H/Cr ratios. The H/Cr ratios are also presented in Table 2 for the same series of CrNb samples. With an initial increase in chromium oxide loading, till 3% Cr_2O_3 loading, the H/Cr ratio is ∼1.7. However, when the chromium oxide loading was further increased the H/Cr ratio decreased from 1.7 for the 3% CrNb sample to 0.6 for the 5% CrNb sample.

Table 2
T_{max} and H/Cr values from TPR studies over Cr_2O_3/Nb_2O_5 samples

Sample	T_{max} (K)	H/Cr
1% CrNb	588	1.8
2% CrNb	594	1.7
3% CrNb	599	1.7
4% CrNb	593	0.9
5% CrNb	594	0.6

3.6. ODH of propane

The ODH of propane was carried out over the CrNb samples at 673, 683, 703 and 723 K. Reaction temperatures above 723 K were not considered since the Nb_2O_5 support is known to be unstable, which would result in the loss of the active sites [18]. At each reaction temperature the propane conversion and propene

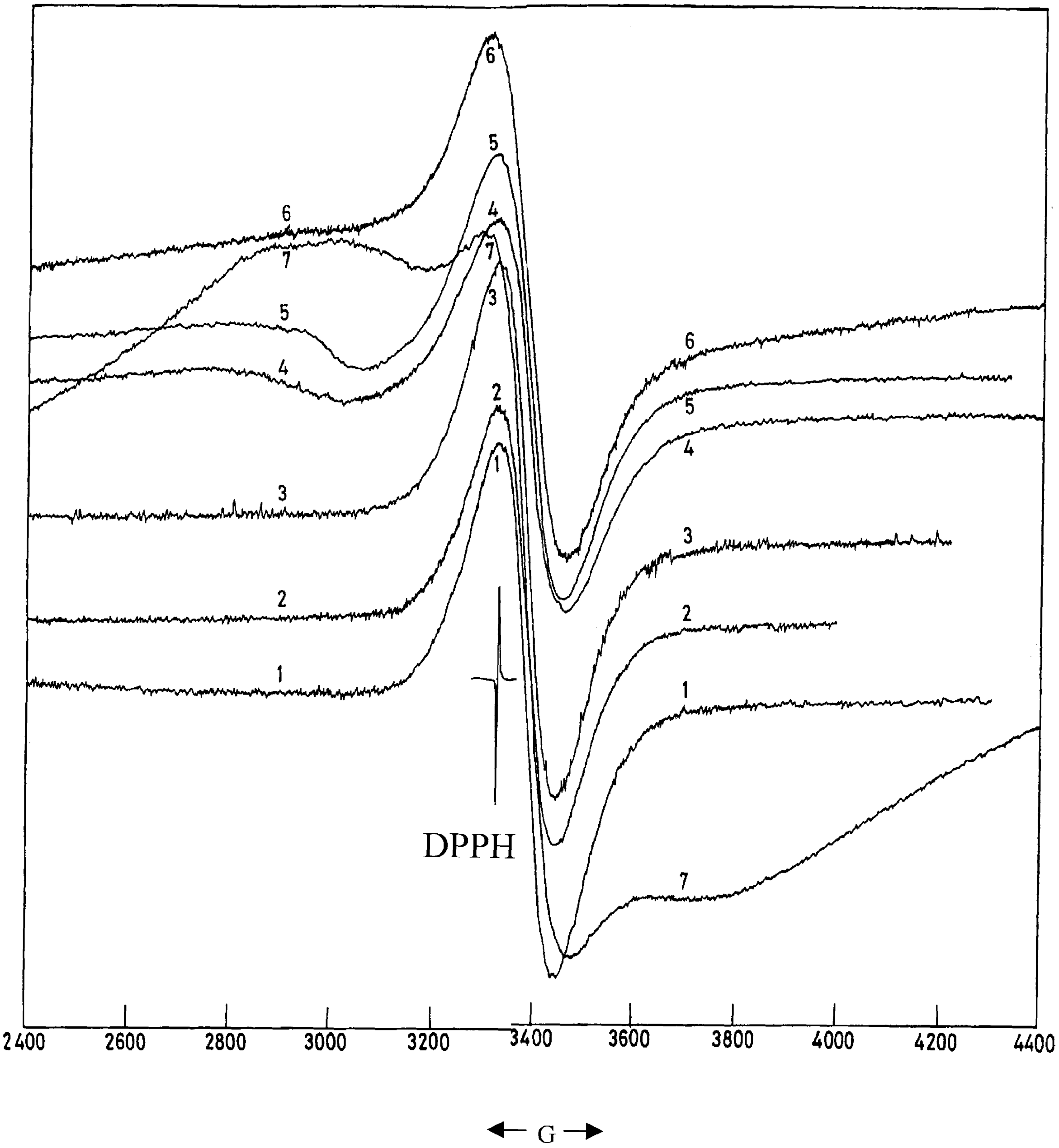

Fig. 3. EPR spectra of the *x*% CrNb catalysts. Legends are as follows: (1) 1%, (2) 2%, (3) 3%, (4) 4%, (5) 5%, (6) 7%, (7) 10%. EPR spectra of DPPH is also included.

selectivity are plotted against chromium oxide loading in Fig. 4. The conversion versus loading curves reveal that with an increase in loading the conversion initially increases and after reaching a maximum conversion for the 3% CrNb sample the conversion decreases for higher chromium oxide loading. This trend in conversion versus chromium oxide loading was observed to be true at all temperatures considered in the present

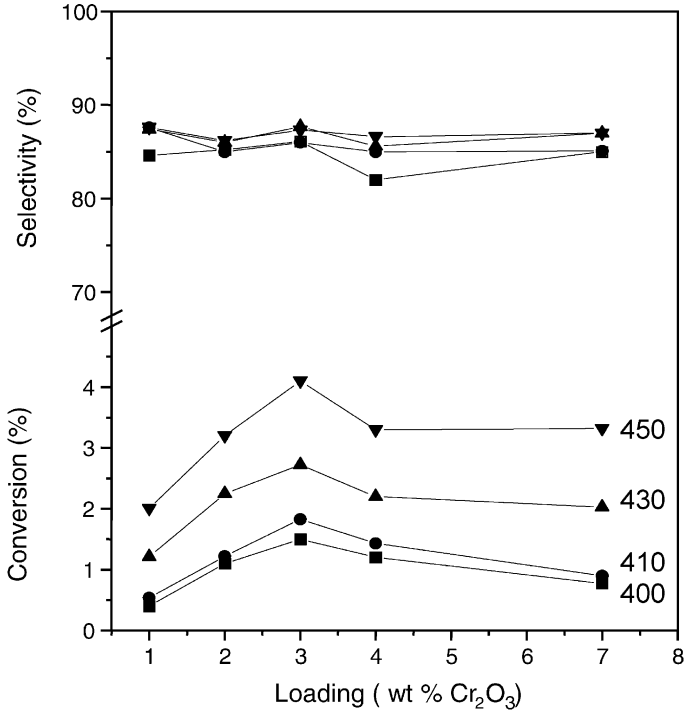

Fig. 4. Conversion and selectivity versus loading for x% CrNb catalysts at different temperature.

study. The selectivity versus loading curves in Fig. 4 reveal that the propene selectivity is not significantly affected by chromium oxide loading. A relatively constant propene selectivity of 82–88% is observed for the CrNb samples.

At 673 K reaction temperature the conversion data are normalized per active site assuming that all chromium oxide sites are taking part in the reaction and represented as TOF (s^{-1}). The TOF values for the 1–7% CrNb samples are presented in Table 3 along with the activity and propene selectivity data. The variations of activity and selectivity are discussed above. Comparison of the TOF values reveal that the TOF is relatively constant for the 1–3% CrNb samples and then decreases for the 4 and 7% CrNb samples. At 683 K reaction temperature a similar variation of TOF with loading is observed. However, at higher temperatures, of 703 and 723 K, the TOF values decrease continuously with loading.

Table 3
Reactivity data for x% CrNb catalysts at 673 K

Sample	Activity × 10^6 (mol/g cat. s)	Selectivity (%)	TOF (s^{-1})
1% CrNb	0.41	85	3.1
2% CrNb	1.14	85	4.4
3% CrNb	1.6	86	4.1
4% CrNb	1.25	82	2.3
7% CrNb	0.83	85	0.9

To study the effect of additives, tungsten and molybdenum oxides were separately added to a previously prepared 1% CrNb sample. The ODH of propane was carried out over these modified 1% Cr_2O_3/Nb_2O_5 samples under the same reaction conditions and the reactivity data are presented in Table 4. Examination of Table 4 reveals that at all reaction temperatures considered the activity for the modified 1% CrNb samples are different than the parent 1% CrNb sample. For the tungsten oxide modified sample, CrNb–4% W, the activity decreases with the addition of tungsten oxide but the propene selectivity slightly increases. The propene yield is also less than the parent 1% CrNb sample. However, with addition of molybdenum oxide, CrNb–2% Mo, the activity and propene

Table 4
Reactivity data for unmodified and modified 1% Cr_2O_3/Nb_2O_5 catalysts

Temperature (K)	Reactivity data	Catalyst		
		1% CrNb	CrNb–4% W	CrNb–2% Mo
673	Activity × 10^6[a]	0.41	0.21	0.36
	Yield (%)	0.3	0.16	0.3
	Selectivity (%)	80	84	83
683	Activity × 10^6[a]	0.56	0.25	0.73
	Yield (%)	0.43	0.21	0.6
	Selectivity (%)	80	87	83
703	Activity × 10^6[a]	1.26	0.83	1.8
	Yield (%)	1.0	0.7	1.5
	Selectivity (%)	83	85	87
723	Activity × 10^6	2.1	1.35	2.5
	Yield (%)	1.7	1.1	2.1
	Selectivity (%)	85	90	86

[a] Activity in terms of moles of C_3H_8 converted per gram catalysts per second.

selectivity slightly increases. The propene yield also increases for the molybdenum oxide modified sample.

4. Discussion

In supported metal oxide catalysts the active metal oxide species form a two-dimensional overlayer on the surface of a high surface area oxide supports. The oxide supports commonly used are alumina, titania, and silica. To confirm the presence of the surface metal oxide species several characterization techniques have been used. In the present study the characterization techniques include Raman, EPR and XPS. The Raman spectra of the CrNb samples reveal the presence of surface chromium (6+) oxide species similar to those observed on the more commonly used supports [11]. Data from XPS studies reveal typical plots that confirm the presence of surface chromium oxide species [19].

Molecularly dispersed surface metal oxide species are the only type of species present on the oxide support on well-prepared samples up to monolayer loadings. Above monolayer loadings crystals of the surface metal oxide species, if stable (e.g., Re_2O_7 is not stable [13]), are formed in addition to the molecularly dispersed species. In the present study crystals of Cr_2O_3 are formed for the 3% CrNb sample, which is evident by the Raman peaks at 550 cm^{-1}. Presence of crystals of Cr_2O_3 also results in the plateauing of the XPS plots in Fig. 2. Consequently, monolayer coverage is exceeded for the 3 wt.% CrNb sample. This Cr_2O_3 loading corresponds to ~11 μmol Cr/m^2. The monolayer loading on the Nb_2O_5 support compares favorably with chromium oxide supported on Al_2O_3 and TiO_2 where ~8 and ~9 μmol of Cr/m^2 are achieved as monolayer coverages [20].

In addition to the surface chromium oxide (6+) species present on the Nb_2O_5, Al_2O_3 and TiO_2 supports, a Cr^{5+} and a dispersed Cr^{3+} species are also present. The Cr^{5+} species are observed in the EPR spectra of the CrNb samples with the EPR parameters as g-value $= 1.97$ and $\Delta H = 110$ G. Similar features are observed with the Cr^{5+} species on the Al_2O_3 and TiO_2 supports [21]. The EPR features of the Cr^{5+} species on Nb_2O_5 are, however, slightly broader which suggests a more distorted Cr^{5+} species. The dispersed Cr^{3+} species is different from the β-Cr^{+3} species observed due to the Cr_2O_3 crystals.

The characterization studies reveal that molecularly dispersed chromium oxide are present on the Nb_2O_5 support, which are similar to those present on more traditional supports, such as, Al_2O_3 and TiO_2. In addition to the surface Cr^{6+} chromates, a Cr^{5+} species is also present on these oxide supports that is readily detected by EPR. However, the chromium (6+) oxide species are the predominant surface species present [22]. Under dehydrated conditions the surface chromates are presented as monochromates and polychromates with a single Cr=O bond on the different oxide supports [11,21]. The ratio of mono- and polychromates do not change with loading for a specific oxide support, but appear to change from one oxide support to another.

The Nb_2O_5 support is also capable of supporting other metal oxide species [3]. These surface metal oxide species are formed usually in their highest oxidation states. Monolayer coverages of other metal oxide species are achieved on Nb_2O_5 support that is comparable to other oxide supports. For example, monolayer coverages of vanadium and molybdenum on Nb_2O_5 are $\sim$14 μmol V^{5+}/m^2 [23] and $\sim$8 μmol Mo^{6+}/m^2 [24], which compare well with monolayer coverages obtained on other oxide supports. Thus, the surface metal oxide species are formed on the Nb_2O_5 support that is similar to those present on other oxide supports.

The surface metal oxide species reveal typical reduction characteristics on commonly used supports as revealed from TPR studies [4,12,13]. In the present study the surface chromium oxide species reveal a single reduction peak (T_{max}) suggesting a single step reduction under the present conditions. The T_{max} temperature is essentially constant at $\sim$623 K. The surface chromium oxide species on Al_2O_3 and TiO_2 supports possess a single reduction peak at $\sim$633 and $\sim$663 K, respectively. The difference in T_{max} temperature is due to the difference in the Cr–O–support bond strength and not due to differences in structure, which is in agreement with previous studies on other supported metal oxide catalysts [4,13]. Furthermore, the H/Cr ratio for the surface chromium oxide species on the Nb_2O_5 support is similar to the H/Cr values observed for the surface CrO_x species on the Al_2O_3 and TiO_2 supports. The TPR studies reveal that surface chromium oxide species on the Nb_2O_5 support is also reducible and the reduction characteristics are due to the Cr–O–support bond. Furthermore, TPR studies on supported vanadium and molybdenum oxide catalysts reveal that the bridging M–O–Nb ($M = V$ or Mo) is responsible for the reduction properties [8]. The structural difference of the specific surface metal oxide species, i.e., vanadium or molybdenum oxides, that arises due to loading does not influence the reduction. Thus, the Nb_2O_5 support is stable for forming the surface metal oxide species with structure similar to those obtained on other oxide supports and reduction properties controlled by the strength of the M–O–Nb bond.

The surface metal oxide species on various supports are the active sites for several reactions [25]. The present study shows that the surface chromium oxide species on Nb_2O_5 is also active for the ODH of propane to propene. The reactivity data reveals that activity for the CrNb catalysts increases with chromium oxide loading up to 3% Cr_2O_3 and decreases with a further increase in chromium oxide loading. From characterization studies crystals of Cr_2O_3 are formed above 3% Cr_2O_3 loading. Crystals of Cr_2O_3 are known to be less active than the surface chromium oxide species [12], and consequently the activity decreases. This behavior is prevalent at all reaction temperatures used in the present study.

The efficiency for the ODH of propane of each surface metal oxide site is given by the TOF. As observed in Table 3, the TOF for the ODH of propane is relatively constant for the surface chromium oxide species. Similar trends were observed for the surface chromium oxide species on the Al_2O_3 and TiO_2 supports. Relating the TOF with structural information suggests that monomeric or polymeric chromium oxide species are equally active for the ODH reaction. Comparing the TOF values of the surface chromium oxide species on the different oxide supports reveal that the values vary as CrNb $\sim$ CrTi $\sim$ CrSi $>$ CrAl $>$ CrSiAl [21]. Thus, the efficiency of the surface chromium oxide species on Nb_2O_5 in converting propane is comparable to that obtained on the best supports, TiO_2. The SiO_2 support is not considered since only small amounts of surface chromium oxide species can be formed [21,26].

The propene selectivities of the CrNb catalysts were high and ranged from 82 to 88%. There was apparently no influence of chromium oxide loading on selectivity. In comparison for Cr_2O_3/Al_2O_3 and Cr_2O_3/TiO_2 catalysts the propene selectivities increased with chromium oxide loading till monolayer coverages [21]. The increase in selectivity is due to the decrease in the exposed Al_2O_3 and TiO_2 surface, which degrades propene. The relatively high and constant propene selectivities suggest that the Nb_2O_5 support does not degrade propene. Since the selectivities are high the propene yields were also consistently high for the CrNb catalysts. Thus, the TOF and yields of propene for the CrNb catalysts suggest that the surface chromium oxide species is comparable, if not better, than values obtained on other oxide supports.

Surface vanadium and molybdenum oxide species on Nb_2O_5 support also show propane ODH activity [8]. Furthermore, tungsten oxide on Nb_2O_5 supports is inactive for propane ODH. Similar to the CrNb system the ODH activity increases for the V_2O_5/Nb_2O_5 and MoO_3/Nb_2O_5 catalysts up to monolayer coverages and then decreases [8]. From the activity data the TOF of the surface vanadium and molybdenum oxide species is also relatively constant. The ratios of different surface vanadium and molybdenum oxide structures appear to change with loading [27]. The relatively constant value of the TOF and the variation of the surface metal oxide structures suggest that the ODH of propane is essentially structure insensitive. This observation is in agreement with unimolecular reactions being structure insensitive [23]. Furthermore, comparison of the TOF values for the niobium oxide supported chromium, vanadium and molybdenum oxide catalysts reveal the following trend: TOF of V_2O_5/Nb_2O_5 $\sim$ TOF of Cr_2O_3/Nb_2O_5 $>$ TOF of MoO_3/Nb_2O_5 $>$ WO_3/Nb_2O_5. The above trend in TOF values for the three different catalysts is different from the TOF values obtained for the ODH of methanol to formaldehyde, where the TOF of V_2O_5/TiO_2 $>$ TOF of MoO_3/TiO_2 $>$ TOF of Cr_2O_3/TiO_2 [28]. The different trends in TOF values observed for the ODH of propane and methanol suggest that the controlling factors in these two reactions are different. Indeed the optical basicity, Λ, which represents the Lewis acidity of the solid plays an important role in the ODH of propane [29,30]. Co-relation reveals that Λ varies as V $\sim$ Cr $>$ Mo $>$ W. The same trend is observed in the TOF of the Nb_2O_5 supported vanadium, chromium, molybdenum and tungsten oxide catalysts. Hence, the TOF for ODH of propane appears to follow the trends of optical basicity.

Additives play an important role in heterogeneous catalysis. Previous studies revealed that there are essentially two types of interactions that occur between the additives and the surface metal oxide species [31]. In the first type of interactions the additives do not affect the structure of the surface metal oxide species and are classified as non-interacting additives. These additives include oxides of niobium, tungsten, silica and vanadium. Consequently, the reactivity of unimolecular simple reactions are not affected when the additives are themselves inactive [31]. However, the additive oxides significantly affect the acid–base characteristics of the supported metal oxide catalysts, which is reflected in the reactivity of more complex reactions [32]. The other class of additives, referred to as interacting additives, directly co-ordinate to the surface metal oxide species and affect the structure and reactivity of the modified supported metal oxide catalysts. Examples of the second type of additives include alkali metal oxides and phosphorous oxides.

In the present work the effect of additives on 1% CrNb catalysts was studied. The additives chosen were molybdenum and tungsten oxides. The loadings chosen were such that the combined coverage of chromium oxide and the additive was less than monolayer coverages. Indeed ambient Raman spectra of the modified 1% CrNb catalysts revealed the absence of crystals of Cr_2O_3, MoO_3, or WO_3. Furthermore, the ambient Raman spectra revealed features of surface chromium and molybdenum oxide or surface chromium and tungsten oxide species. The TPR studies of molybdenum oxide modified 1% CrNb catalysts reveal two reduction peaks corresponding to the surface chromium and molybdenum oxide, respectively. The TPR studies on tungsten oxide modified 1% CrNb catalysts were not successful and only a small reduction peak for the surface chromium oxide species is observed. The behavior of tungsten oxide on CrNb samples is similar to the tungsten oxide on CrTi and CrAl samples with respect to the Raman spectra [17]. In these sample the surface tungsten oxide species did not interact with the surface chromium oxide species. Similar to these studies the surface tungsten oxide appears to be irreducible in the experimental conditions considered in the present study. Thus, the characterization studies reveal that molybdenum and tungsten oxide additives do not affect the structure or reducibility of the surface chromium oxide species.

The reactivity of the modified 1% CrNb samples reveals different behavior. The tungsten oxide modified 1% CrNb catalyst reveals a decrease in activity, whereas, the molybdenum modified 1% CrNb catalyst reveals a slight increase in activity. The surface tungsten oxide species do not form surface redox sites and are inactive for the ODH of propane under the present experimental conditions. However, the acid–base properties of the catalyst are modified with the addition of surface tungsten oxide. For tungsten oxide modified vanadia–titania catalysts the Bronsted acidity increased, whereas, the Lewis acidity primarily arising from the support decreases [33]. Previous studies have proposed that the Lewis acidity plays an important role in the ODH activity [34]. Hence, it appears that the addition of surface tungsten oxide decreases the Lewis acidity, and, consequently, decreases the adsorption of propane, which is reflected in the decrease in activity. Addition of surface molybdenum oxide results in an increase in activity, which is primarily due to the redox activity of the surface molybdenum oxide species. Thus, it appears that both the molybdenum and tungsten oxide modifiers behave as non-interacting additives and change the ODH of propane activity by affecting the acid–base and redox characterization of the modified catalysts in different ways.

5. Conclusion

Niobium oxide supported chromium oxide catalysts, CrNb, was used as a representative supported metal oxide catalyst for the ODH of propane to study the advantage of using Nb_2O_5 as a support material. Several loadings of chromium oxide on Nb_2O_5 were prepared and characterized by Raman, TPR and XPS. The presence of surface chromium oxide species was detected below monolayer coverages, which was achieved at surface concentrations below 11 μmol Cr/m^2. Monolayer coverage values compare well with other supported chromium oxide catalysts, such as, Cr_2O_3/TiO_2 and Cr_2O_3/Al_2O_3. The structure of the surface chromium oxide species appears to be similar on the Nb_2O_5, Al_2O_3 and TiO_2 supports. The reducibility of the surface chromium oxide species on Nb_2O_5 was, however, different from the reducibility of the surface chromium oxide species on the other oxide supports (TiO_2 and Al_2O_3). The difference in reducibility appears to be due to the difference in the Cr–O–support bond strength and not due to structural difference of the surface chromium oxide species.

The surface chromium oxide species on Nb_2O_5 was active for the ODH of propane and propene was the main product formed with selectivities greater than 80% in the temperature range 673–723 K. Furthermore, each surface chromium oxide species appears to be equally active for converting propane. Similar results have been observed for the surface chromium oxide species on Al_2O_3 and TiO_2 supports. The TOF of the surface chromium oxide species on Nb_2O_5 was comparable to the value obtained on TiO_2 and better than the value obtained on Al_2O_3. The propene selectivities of the Cr_2O_3/Al_2O_3 and Cr_2O_3/TiO_2 catalysts, however, increase with loading since the amount of exposed surface decreases. The high propene selectivities on CrNb catalysts irrespective of loading suggest that the Nb_2O_5 support does not degrade propene as much as the Al_2O_3 and TiO_2 supports. The effect of non-interacting additives, molybdenum and tungsten oxide, was also studied. A marginal increase in activity was observed for the molybdenum oxide modified CrNb catalyst but no increase in activity was observed for the tungsten oxide modified CrNb catalysts. The marginal increase was due to the small redox activity of the surface molybdenum oxide species under the present reaction conditions. It appears that increasing the Bronsted acidity does not increase the ODH activity.

Other surface metal oxide species are also formed on Nb_2O_5 supports. Monolayer coverages of these metal oxides are also comparable with values obtained on other oxide supports. The reducibility of the surface metal oxide species is controlled by the strength of the M–O–niobium oxide bond, where M is the metal of the surface metal oxide species. The TOF of other surface metal oxide species on Nb_2O_5 are relatively constant with respect to loading, similar to the surface chromium oxide species on Nb_2O_5. The different Nb_2O_5 supported metal oxide species have TOF that vary as follows: $V \sim Cr > Mo > W$. The difference in TOF values appears to be related to the optical basicity. The propene selectivities of these surface metal oxide species on the Nb_2O_5 support were also high. Thus, niobium oxide is a promising support material for making effective supported metal oxide catalysts that can be used for the ODH reaction since high TOF and propene selectivity are obtained.

Acknowledgements

The authors gratefully acknowledge A.M. Hirt for providing the XPS data and Prof. I.E. Wachs for providing the Raman data. This work has been partially supported by the financial assistance of The Department of Science and Technology, India.

References

[1] B. Delmon, P. Ruiz, S.R.G. Carrazan, S. Korili, M.A. Vicente Rodriguez, Z. Sobalik, Catal. Petrol. Ref. Petrochem. Ind. (1995) 1.

[2] S. Kasaoka, E. Sasaoka, H. Iwasaki, Int. Chem. Eng. 4 (1994) 431.

[3] J.M. Jehng, A.M. Turek, I.E. Wachs, Appl. Catal. 83 (1992) 179.

[4] G. Deo, I.E. Wachs, J. Catal. 129 (1991) 307.

[5] I.E. Wachs, J.M. Jehng, G. Deo, H. Hu, N. Arora, Catal. Today 28 (1996) 199.

[6] R.H.H. Smits, K. Seshan, H. Leemreize, J.R.H. Ross, Catal. Today 16 (1993) 513.

[7] T.C. Watling, G. Deo, K. Seshan, I.E. Wachs, J.A. Lercher, Catal. Today 28 (1996) 139.

[8] Z. Zhao, I.E. Wachs, Abstracts of Papers, in: Proceedings of the 222nd ACS National Meeting, Chicago, IL, August 26–30, 2001.

[9] F.D. Hardcastle, I.E. Wachs, J. Mol. Catal. 46 (1988) 173.

[10] M. Cherian, M.S. Rao, G. Deo, CHEMINAR, 2001, Bhubaneswar, India.

[11] M.A. Vuurman, D.J. Stufkens, A. Oskam, J.A. Moulijn, F. Kapteijn, J. Mol. Catal. 60 (1990) 83.

[12] M. Cherian, M.S. Rao, W.T. Yang, J.M. Jehng, A.M. Hirt, G. Deo, Appl. Catal. A 233 (2002) 21.

[13] B. Mitra, X. Gao, A.M. Hirt, I.E. Wachs, G. Deo, Phys. Chem. Chem. Phys. 3 (2000) 1144.

[14] M.A. Vuurman, I.E. Wachs, A.M. Hirt, J. Phys. Chem. 95 (1991) 9928.

[15] B.M. Weckhuysen, I.E. Wachs, A. Schoonheydt, Chem. Rev. 96 (1996) 3327.

[16] S. Khaddar-Zine, A. Ghorbel, C. Naccache, J. Mol. Catal. 150 (1999) 223.

[17] M. Cherian, R. Gupta, M.S. Rao, G. Deo, Catal. Lett., Studies in Surface Science and Catalysis, vol. 100, Elsevier, Amsterdam, 1996, p. 1.

[18] I.E. Wachs, L.E. Briand, J.M. Jehng, L. Burcham, X. Gao, Catal. Today 57 (2000) 323.

[19] Ch. Fountzoula, H.K. Matralis, Ch. Papadopoulou, G.A. Voyiatzis, Ch. Kordulis, J. Catal. 172 (1997) 391.

[20] M. Cherian, M.S. Rao, G. Deo, CHEMCON-2002, Chennai, India.

[21] M. Cherian, M.S. Rao, A.M. Hirt, I.E. Wachs, G. Deo, J. Catal. 211 (2002) 482.

[22] M.I. Zaki, N.E. Fouad, G.C. Bond, S.F. Tahir, Thermochim. Acta 285 (1996) 167.

[23] G. Deo, I.E. Wachs, J. Haber, Crit. Rev. Surf. Chem. 4 (1994) 141.

[24] H. Hu, I.E. Wachs, J. Phys. Chem. 99 (1995) 10911.

[25] I.E. Wachs, J.M. Jehng, G. Deo, B.M. Weckhuysen, V.V. Guliants, J.B. Benziger, Catal. Today 32 (1996) 47.

[26] D.S. Kim, J.M. Tatibouet, I.E. Wachs, J. Catal. 136 (1992) 209.

[27] M.A. Vuurman, I.E. Wachs, J. Phys. Chem. 96 (1992) 5008.

[28] I.E. Wachs, G. Deo, M.A. Vuurman, H. Hu, D.S. Kim, J.M. Jehng, J. Mol. Catal. 82 (1993) 443.

[29] P. Moriceau, A. Lebouteller, E. Bordes, P. Courtine, Phys. Chem. Chem. Phys. 1 (1999) 5735.

[30] P. Moriceau, B. Taouk, E. Bordes, P. Courtine, Catal. Today 61 (2000) 197.

[31] G. Deo, I.E. Wachs, J. Catal. 146 (1994) 335.

[32] I.E. Wachs, J.M. Jehng, G. Deo, B.M. Weckhuysen, V.V. Guliant, J.M. Benziger, S. Sundaresan, J. Catal. 170 (1997) 75.

[33] I.E. Wachs, G. Deo, B.M. Weckhuysen, A. Andreini, M.A. Vuurman, M. de Boer, M.D. Amiridis, J. Catal. 161 (1996) 211.

[34] K. Chen, A.T. Bell, E. Iglesia, J. Phys. Chem. 104 (2000) 1292.